Gradient Flow in 2D XY model

Mainak Pal

Indian Association for the Cultivation of Science

August 11, 2020

Abstract

The gradient flow method is proposed as a method of estimating density of free topological defects in 2D XY model and its validity is checked against Kosterlitz-Thouless vortex unbinding picture.

Contents

1 Introduction

Recently there has been much interest in estimating the density of free topological defects in lattice models. This is because in systems which exhibit a topological phase transition the density of free topological defects play very important role both in equilibrium and non-equilibrium scenarios[1]. One such interesting model is the 2D XY model. This model does not have a conventional order disorder thermal phase transition described by local order parameter. Instead it has a topological phase transition. Renormalization group calculations done on continuum version of this model by Kosterlitz and Thouless [2] show that at temperatures below a certain transition temperature T_{BKT} (Berezinskii,Kosterlitz,Thouless temperature) the vortices and anti-vortices are bound together to form a dipole and only at higher temperatures there exists free vorties. Naturally it is also important to know how things work out in finite size lattices. So far the numerical estimates of defect density in finite system sizes have been of an ad hoc nature (see [1]). There also have been some machine learning studies trying to find free vortices using sophisticated numerical tools such as convolutional neural networks. [3]

In our work we try to construct a simple course graining method. The method we propose is motivated by gradient flow or Wilson flow method introduced in Lattice QCD by Martin Lüscher[4]. The Wilson flow method is used as a coarse graining procedure on gauge configurations generated by numerical simulations. The gauge configurations generated at finite flow time are smooth renormalized field configurations. We use the gradient flow method in a similar manner to coarse grain the spin configurations generated by Monte Carlo simulations and try to obtain the density of free topological defects left over after coarse graining.

The 2D XY model shows a peculiar phase transition. According to the Mermin-Wagner theorem the 2D XY model cannot have long range order at any finite temperature (however small). This is because spin-wave excitations or Goldstone modes (which require infinitesimally small amount of energy) destroy the long range ordering and the system only has quasi long range order (QLRO) at low temperatures. It is in contrast with other conventional models of phase transitions with discrete degrees of freedom such as the 2D Ising model which has a long range ordered ferromagnetic phase and exhibits a second order phase transition to a disordered paramagnetic phase. This can in part be attributed to the discrete nature of the spins and the fact that any excitation requires a finite amount of energy in Ising model, unlike our 2D XY model. In the QLRO phase the spin-spin correlation functions show power law decay, but at high temperatures the nature of correlation function changes and they decay in an exponential fashion. This signals that there should be some kind of phase transition happening at intermediate temperatures, albeit not of a symmetry breaking nature.

Although the Mermin-Wagner theorem prohibits any symmetry breaking phase transition, there has been considerable evidence of a phase transition in 2D XY model from experiments on thin superfluid films as well as from numerical Monte Carlo simulations.

The contradictions were resolved mainly due to Berezinski,Kosterlitz and Thouless who argued from a renormalization group point of view that although there is no symmetry breaking phase transition, there is still a new kind of topological phase transition driven by proliferation of excitations such as vortices and anti-vortices. They showed that in the low temperature phase vortices and anti-vortices are tightly bound together but at high temperatures they unbind and become free. This kind of phase transition is exciting in the sense that it is not described by a local order parameter as in conventional Landau-Ginzburg theory, but rather depends on global properties of the system.

2 2D XY Model and the BKT transition

The 2D XY model is defined by a set of classical planar rotors $\vec{S}(x)$ whose directions are parametrized by angular variables $\theta(x)$ living on a square lattice Λ having L sites in both directions. The angles $\theta(x) \in [0, 2\pi)$ are defined w.r.t the +ve X axis of the lattice. This choice is arbitrary and all choices are equivalent. These planar rotors or spins interact with their neighbours via the following Hamiltonian

$$\mathcal{H} = -J \sum_{\langle xy \rangle} \vec{S}(x) \cdot \vec{S}(y) = -J \sum_{\langle xy \rangle} \cos(\theta(x) - \theta(y)) \tag{2.1}$$

Where the sum is over the pair of all first nearest neighbour sites.

2.1 Non-linear Sigma Model

The instability of the ordered state in 2D XY model can be explained by looking at the fluctuation of the Goldstone modes of n component spins in a d dimensional lattice, i.e.

$$\vec{s}(x) = (s_1(x), s_2(x), ..., s_n(x)) \text{ with } |\vec{s}(x)| = 1 \tag{2.2}$$

A possible ground state of this model is $\vec{s}(x) = (0, 0, ..., 1)$. Corresponding to this ground state there are $n - 1$ Goldstone modes. If we consider small fluctuations about this ground state we have

$$\vec{s}(x) = (\vec{\pi}_1(x), \vec{\pi}_2(x), ..., \vec{\pi}_{n-1}(x), \sigma(x)) \tag{2.3}$$

We can integrate out the $\sigma(x)$ fields using the constraint $\pi^2(x) + \sigma^2(x) = 1$ and we obtain the following partition function for the Goldstone modes

$$\mathcal{Z}_{\rm G} = \int \mathcal{D}\vec{\pi}(x)\ \exp\left(- \int d^d\vec{x}\ \Big[\frac{K}{2}(\nabla\vec{\pi})^2 + \frac{K}{2}\Big(\nabla\sqrt{1-\pi^2}\Big)^2 - \frac{\rho}{2}\ln(1-\pi^2)\Big]\right) \tag{2.4}$$

Where ρ is the density of lattice sites. If we take into account only the free partition function we get

$$\begin{aligned}\langle|\pi(x)|^2\rangle &= \int \frac{d^d\vec{q}}{(2\pi)^d}\langle|\pi(\vec{q})|^2\rangle_0 = \frac{n-1}{K}\int_{1/L}^{1/a}\frac{d^d\vec{q}}{(2\pi)^d}\frac{1}{q^2} \\ &= \frac{n-1}{K}\frac{K_d}{d-2}\Omega_d\end{aligned} \tag{2.5}$$

Where $\Omega_d(d \neq 2) = a^{2-d} - L^{2-d}$ and $\Omega_d(d = 2) = \ln(L/a)$. This clearly shows that for $d \leq 2$ there is a divergence in the fluctuations of the Goldstone modes and hence the initial ground state in not stable against thermal fluctuations in the thermodynamic limit.

2.2 Coulomb Gas Approximation

At low enough temperatures where the variation in the orientation of the spins are small, the model can be decomposed into spin wave and vortex degrees of freedom. The total partition function can be written as

$$\begin{aligned}\mathcal{Z} &= \int_0^{2\pi}\prod_x \frac{d\theta(x)}{2\pi}\ \exp\Big(K\sum_{\langle xy\rangle}\cos(\theta(x)-\theta(y))\Big) \\ &\propto \mathcal{Z}_{\rm SW}\mathcal{Z}_{\rm Q}\end{aligned} \tag{2.6}$$

Where $\mathcal{Z}_{\rm SW}$ is the partition function for the spin wave excitations

$$\mathcal{Z}_{\rm SW} = \int \mathcal{D}\phi(\vec{r})\exp\Big(-\frac{K}{2}\int d^2\vec{r}\ (\nabla\phi)^2\Big) \tag{2.7}$$

And $\mathcal{Z}_{\rm Q}$ is the same for positive and negative charges interacting via a logarithmic potential $C(\vec{r}_i - \vec{r}_j) = \ln(|\vec{r}_i - \vec{r}_j|)/2\pi$

$$\mathcal{Z}_{\rm Q} = \sum_{\{n_i\}}\int d^2\vec{r}\ \exp\Big(-\sum_i \beta E^0_{n_i} + 4\pi^2 K\sum_{i<j} n_i n_j\ C(\vec{r}_i - \vec{r}_j)\Big) \tag{2.8}$$

$E^0_{n_i}$ denotes the energy of the vortex cores. β is the inverse temperature and $K = \beta J$. At low temperatures we can keep only elementary vortex, anti-vortex excitations with $n_i = \pm 1$ and zero total topological charge, i.e. $\sum_i n_i = 0$.With this further simplification we have

$$\mathcal{Z}_{\mathrm{Q}} = \sum_{N=0}^{\infty} y_0^N \int \prod_{i=1}^{N} d^2\vec{r}\, \exp\left(4\pi^2 K \sum_{i<j} n_i n_j\, C(\vec{r}_i - \vec{r}_j)\right) \tag{2.9}$$

A perturbative RG analysis of this Coulomb gas model gives us RG flow equations for y_0 and K

$$\frac{dK^{-1}}{dl} = 4\pi^3 a^4 y_0^2 + \mathcal{O}(y_0^4) \tag{2.10}$$

$$\frac{dy_0}{dl} = (2 - \pi K) y_0 + \mathcal{O}(y_0^3) \tag{2.11}$$

The solutions to the above RG flow equations imply that at low temperatures (high K^{-1}) and small y_0 the flow terminates on the line $y_0 = 0$ and $K_{\mathrm{eff}} \geq 2/\pi$. In this phase a vortex and an anti-vortex form a dipole like structure and all defects are paired in this manner. Flows which do not terminate on this line reach asymptotically reach higher and higher values of give K^{-1} and y_0 and at very high temperature the perturbative picture breaks down. This means that at high temperature coarse graining does not reduce y_0 to zero and hence there are a large number of free vortices.

3 Gradient Flow

The gradient flow method introduces a new time called *flow time* which is distinct from the MC time and gives new dynamical equations (flow equations) for the degrees of freedom in the system. The flow equations for a system with Hamiltonian $\mathcal{H}$ are given as

$$\frac{d}{d\tau}\theta(x,\tau) = -\frac{\delta\mathcal{H}}{\delta\theta(x,\tau)} \quad \forall x \in \Lambda \tag{3.1}$$

Where τ denotes flow time. For our specific Hamiltonian these equations reduce to

$$\frac{d}{d\tau}\theta(x,\tau) = -J \sum_{y \in nn(x)} \sin(\theta(x,\tau) - \theta(y,\tau)) \quad \forall x \in \Lambda \tag{3.2}$$

We solve the flow equations using Runge-Kutta integration.

4 Heatbath Monte Carlo Sampling

Instead of using the Metropolis algorithm for performing Monte Carlo updates on our system we have used an approximate rejection based heatbath method. It is an approximation in the sense that there is a small amount of rejection of the proposed configurations whereas in a perfect heatbath algorithm all generated configurations are accepted without rejection. Although not perfect, this has the

advantage of having higher acceptance rate compared to standard Metropolis algorithm. Also the autocorrelation time is much shorter which means that we can get smaller error bars with same or fewer Monte Carlo sweeps. We will now describe the formulation of the algorithm below. It is adopted from a similar Monte Carlo update procedure used in $U(1)$ lattice gauge theory.

Let us consider the part of the Hamiltonian associated with the angular variable $\theta(x)$ at site $x \in \Lambda$. It is given by

$$\mathcal{H}[\theta(x)] = -J \ \vec{s}(x) \cdot \vec{h}_{\text{eff}}(x) \tag{4.1}$$

$$\vec{h}_{\text{eff}}(x) = \sum_{y \in nn(x)} \vec{s}(y) \tag{4.2}$$

As we see $\vec{h}_{\text{eff}}(x)$ is the effective magnetic field at site x due to spins sitting at it's first nearest neighbour positions. Let us now define $h_{\text{eff}}(x) = |\vec{h}_{\text{eff}}(x)|$ as the magnitude of this effective field and $\theta_{\text{eff}}(x)$ as it's orientation w.r.t +ve X axis. With this we can rewrite equation (3.1) as

$$\mathcal{H}[\theta(x)] = -Jh_{\text{eff}} \cos(\theta(x) - \theta_{\text{eff}}(x)) \tag{4.3}$$

So in a canonical ensemble at inverse temperature β the probability distribution function of the angular variable $\theta(x)$ will be given as

$$\begin{aligned} p(\theta(x)) &= \exp\{-\beta \mathcal{H}[\theta(x)]\} \\ &= \exp\{\rho \cos(\theta(x) - \theta_{\text{eff}}(x))\} \end{aligned} \tag{4.4}$$

Where we have defined $\rho = \beta J h_{\text{eff}}$. Now, if we could sample a random variable $\theta(x)$ from the distribution $p(\theta(x))$ then we would have effectively constructed an exact heatbath algorithm for the 2D XY model. Sampling from a distribution can be done without rejection using the method of Inverse Transform Sampling, but this requires one to know the cumulative probability distribution function. In other words we would require the following indefinite integral

$$I(a, b) = \int_a^b dz \ e^{\rho \cos(z)} \tag{4.5}$$

The answer to the integral (3.5) is not known. However there is a related function which can be integrated, namely

$$\tilde{I}(a, b) = \int_a^b dz \ \frac{e^{\rho}}{1 + \rho(1 - \cos(z))} \tag{4.6}$$

Knowing the integral (3.6) means that we can sample random numbers from a new distribution function $\tilde{p}(\theta(x))$, where

$$\tilde{p}(\theta(x)) = \frac{e^{\rho}}{1+\rho(1-\cos(\theta(x)-\theta_{\text{eff}}(x)))} \tag{4.7}$$

The two distributions are related in the sense that they have quite similar shape and value of $\tilde{p}(\theta(x))$ is always greater than $p(\theta(x))$ as it can be seen from figure ??? (attach graph). This means that we can sample random numbers from the distribution $\tilde{p}(\theta(x))$ and then reject some of those numbers in such a way that we effectively sample from $p(\theta(x))$.

Using Inverse Sampling Transform, to sample a number z randomly from a probability distribution $F(z)$ we first select a flat random number in the interval $[0,1]$, say u and set

$$u = \frac{1}{N}\int_{z_{\min}}^{z} dz'\ F(z') \equiv G(z) \ \text{ where } \ N = \int_{z_{\min}}^{z_{\max}} dz'\ F(z') \tag{4.8}$$

Then $z = G^{-1}(u)$ will be distributed according to $F(z)$. We now note the following integral

$$\int dz\ \frac{1}{a+b\cos(z)} = \frac{2}{\sqrt{a^2-b^2}}\tan^{-1}\left(\frac{\sqrt{a^2-b^2}\ \tan(z/2)}{a+b}\right); a^2 > b^2 \tag{4.9}$$

Using this for $\tilde{p}(\theta(x))$ we obtain

$$N = \frac{2\pi\, e^{\rho}}{\sqrt{1+2\rho}} \ \text{ and } \ \frac{1}{\sqrt{1+2\rho}}\ \tan\left(\pi u - \frac{\pi}{2}\right) = \tan\left(\frac{z}{2}\right) \tag{4.10}$$

As we have seen above this sampling algorithm uses information from the system such as J,β,$\vec{h}_{\text{eff}}$ to make an educated guess while proposing a new configuration which is quite likely to be accepted.

5 Results

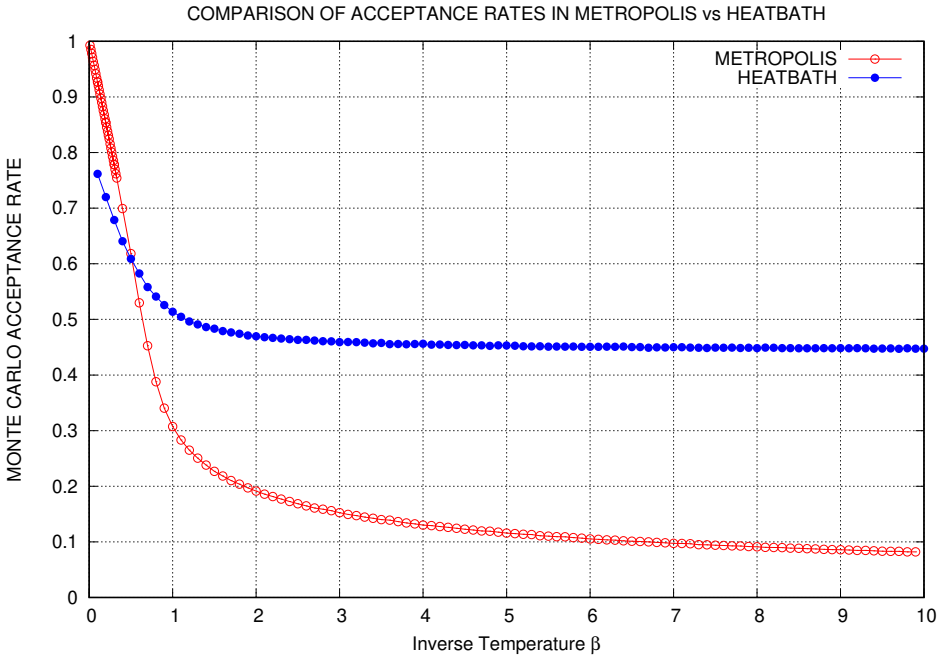
COMPARISON OF ACCEPTANCE RATES IN METROPOLIS vs HEATBATH
METROPOLIS
HEATBATH
MONTE CARLO ACCEPTANCE RATE
Inverse Temperature β
0
0.1
0.2
0.3
0.4
0.5
0.6
0.7
0.8
0.9
1
0
1
2
3
4
5
6
7
8
9
10

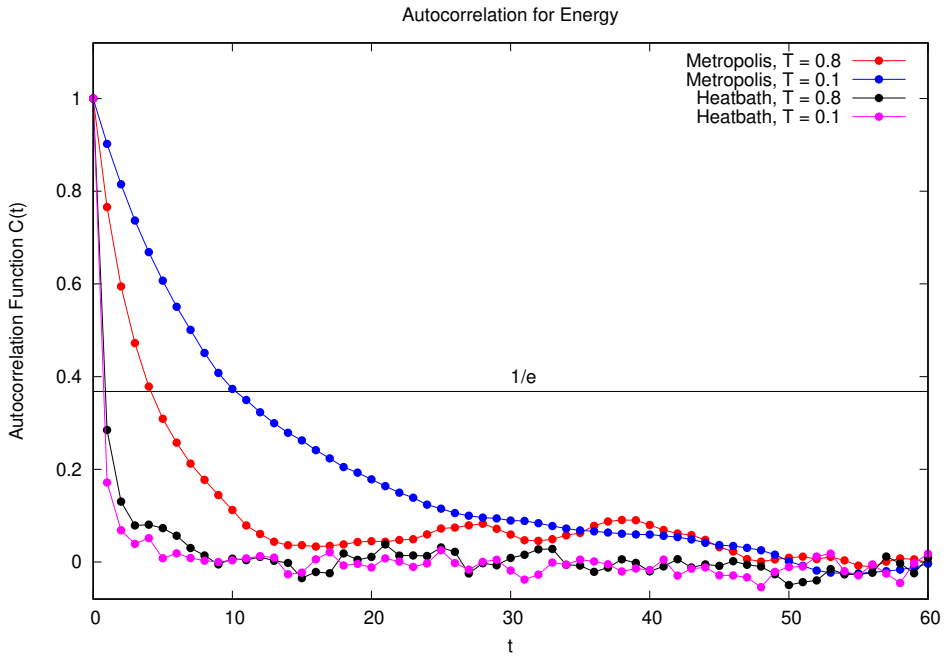
Autocorrelation for Energy
Metropolis, T = 0.8
Metropolis, T = 0.1
Heatbath, T = 0.8
Heatbath, T = 0.1
1/e
Autocorrelation Function C(t)
t
0
0.2
0.4
0.6
0.8
1
0
10
20
30
40
50
60

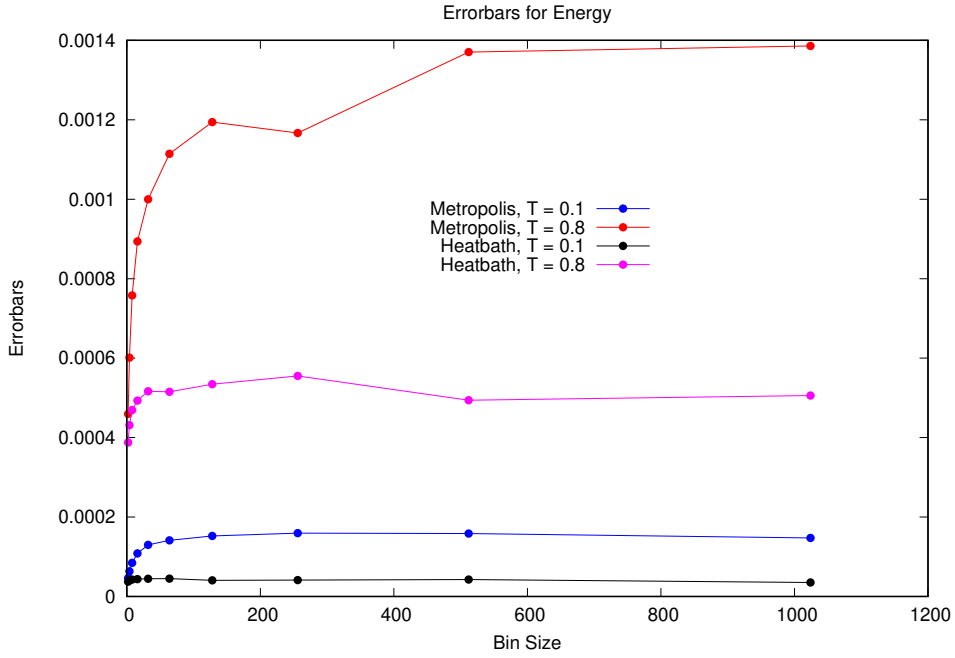
Errorbars for Energy
Metropolis, T = 0.1
Metropolis, T = 0.8
Heatbath, T = 0.1
Heatbath, T = 0.8
Errorbars
Bin Size
0
0.0002
0.0004
0.0006
0.0008
0.001
0.0012
0.0014
0
200
400
600
800
1000
1200

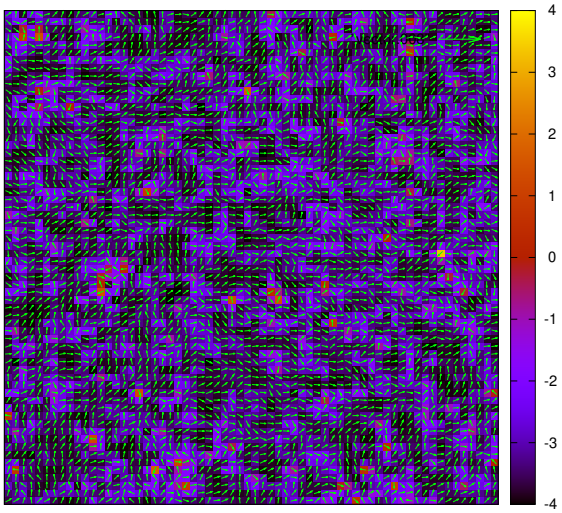

Figure 5.1: Spin configuration at $T < T_{BKT}$ and corresponding energy per site shown as color plot before Gradient Flow

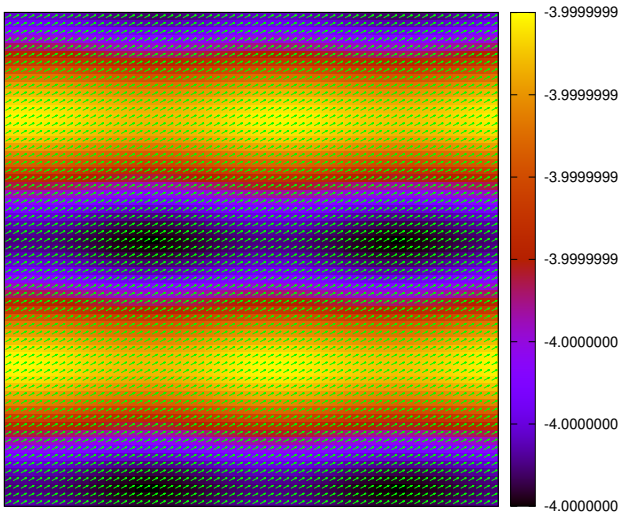

Figure 5.2: Spin configuration at $T < T_{BKT}$ and corresponding energy per site shown as color plot after Gradient Flow. As we can see the initial rough structure of the spins has been smoothed out completely. We have reached the global minima for the spin configuration. There are no spin wave excitations or free vortices present in the system and all the spins are almost parallel

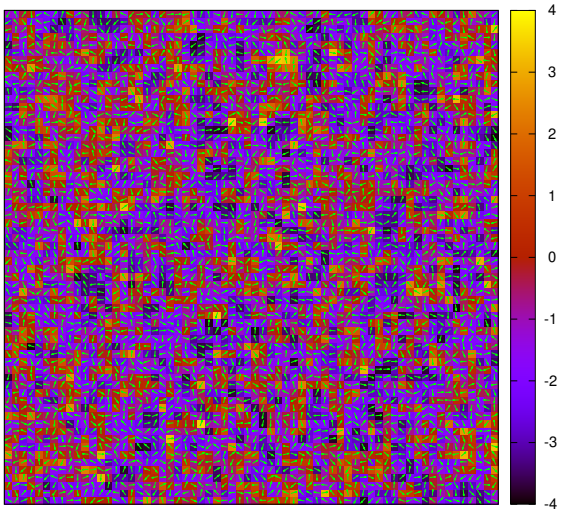

Figure 5.3: Spin configuration at $T > T_{BKT}$ and corresponding energy per site shown as color plot before Gradient Flow.

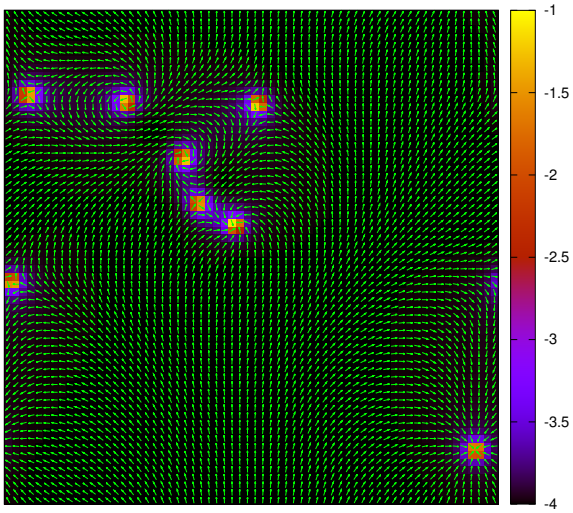

Figure 5.4: Spin configuration at $T > T_{BKT}$ and corresponding energy per site shown as color plot Gradient Flow. Similar to the $T < T_{\mathrm{BKT}}$ case the spin configuration has smoothed out but there are free vortices present. At this stage we are stuck in the local minima of the system.

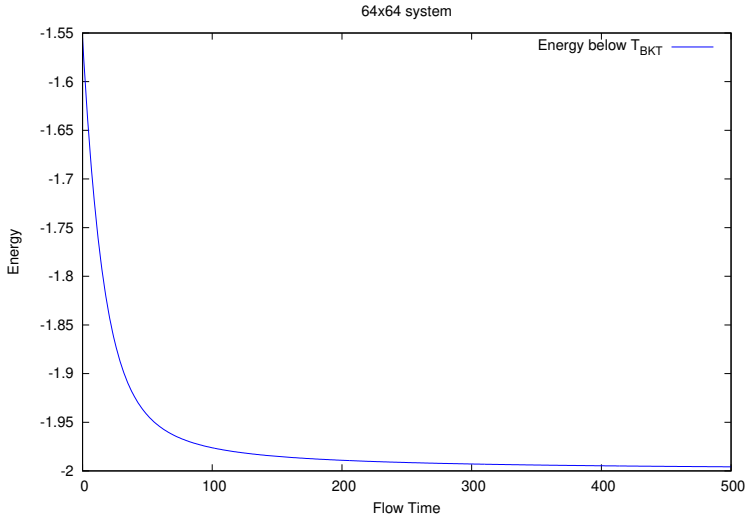

Figure 5.5: Initial state taken from $T < T_{BKT}$.We can see energy decreases in a very smooth fashion and goes very close to global minimum value of -2.

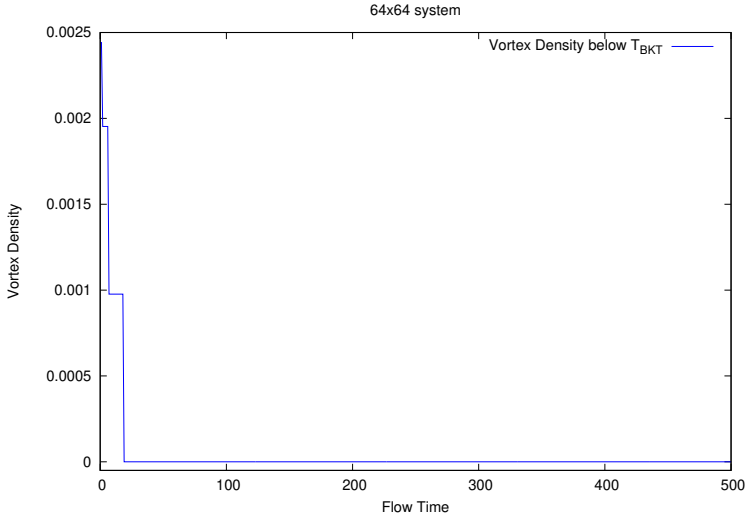

Figure 5.6: Initial state taken from $T < T_{BKT}$. We can see that the vortex density drops to zero very fast. This happens because at low temperature the vortices and antivortices are tightly bound to each other and under Gradient flow they quickl attract each other and annihilate.

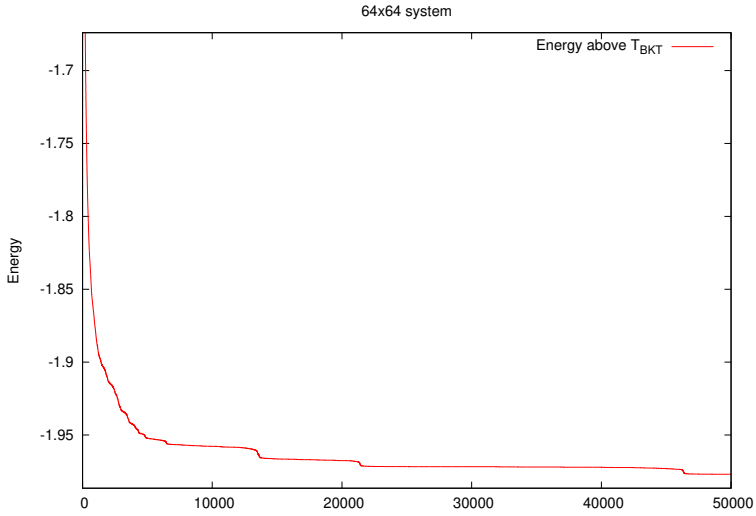

Figure 5.7: Initial state taken from $T > T_{BKT}$. Initially the energy falls almost similar to the $T < T_{BKT}$ case but has some sharp jumps, which are more prominent at later stages of the flow.

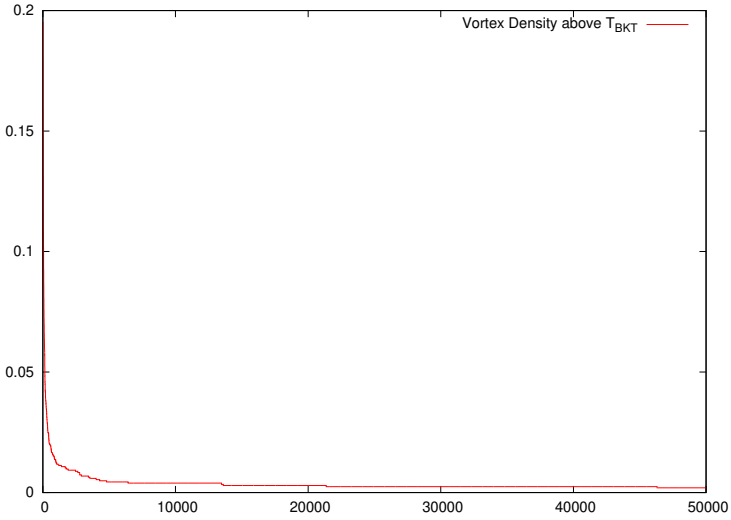

Figure 5.8: Initial state taken from $T > T_{BKT}$. Initially the vortex falls almost similar to the $T < T_{BKT}$ case but has some sharp jumps, which are more prominent at later stages of the flow. The jumps in the energy correspond to this jumps where bound pairs annihilate.

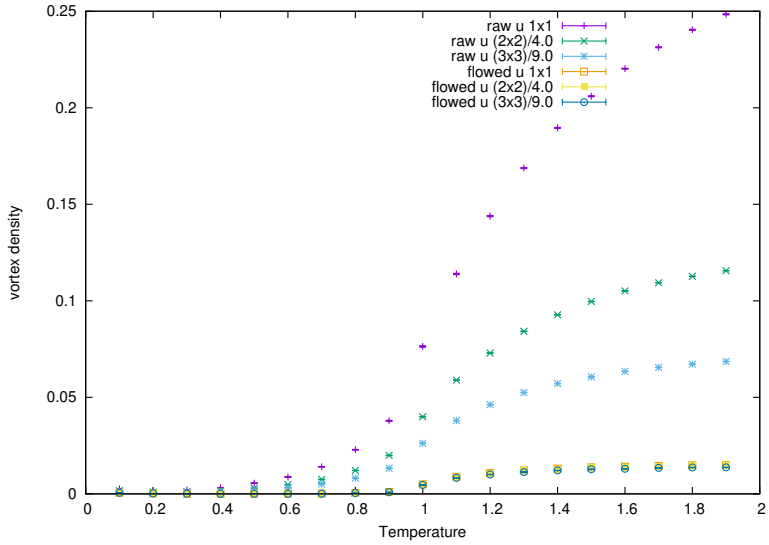

Figure 5.9: Vortex Density before (raw) and after flow(flowed) for different plaquette sizes for a 64×64 system. As we can see the the raw densities are non zero before T_{BKT} and are different from each other. The flowed densities are however only non-zero above T_{BKT} and are almost same.

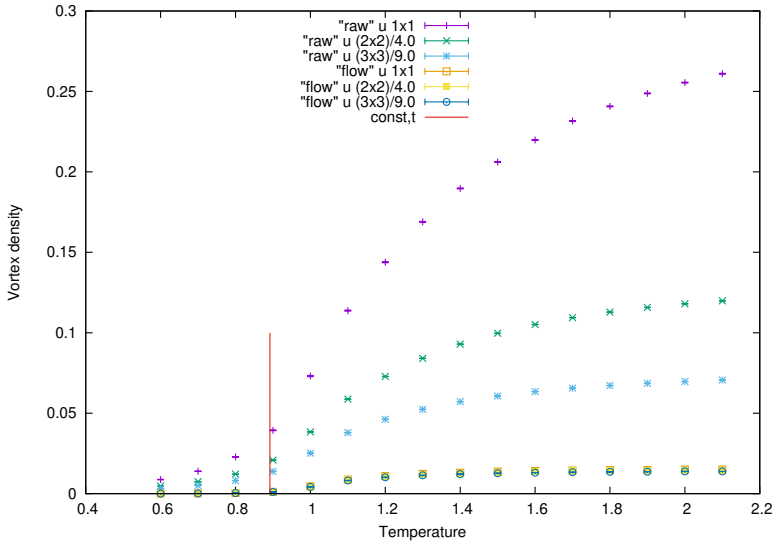

Figure 5.10: Same as figure before but with 128×128 system size. The red vertical line points out the critical temperature.

References

[1] A. Jelić and L. F. Cugliandolo, "Quench dynamics of the 2dxymodel," *Journal of Statistical Mechanics: Theory and Experiment*, vol. 2011, p. P02032, Feb 2011.

[2] J. M. Kosterlitz and D. J. Thouless, "Ordering, metastability and phase transitions in two-dimensional systems," *Journal of Physics C: Solid State Physics*, vol. 6, pp. 1181–1203, apr 1973.

[3] M. J. S. Beach, A. Golubeva, and R. G. Melko, "Machine learning vortices at the kosterlitz-thouless transition," *Physical Review B*, vol. 97, Jan 2018.

[4] M. Lüscher, "Properties and uses of the wilson flow in lattice qcd," *Journal of High Energy Physics*, vol. 2010, Aug 2010.